



HAL
open science

Design of New Partially Bio-Based Polyguanamines for the Reversible Adsorption of Phenolic Molecules from Olive Mill Wastes

Siwar Cherbib, Ibtissem Jlalia, Taha Chabbah, Saber Chatti, Catherine Marestin, Regis Mercier, Stefen Weidner, Herve Casabianca, Nicole Jaffrezic-Renault, Houyem Abderrazak

► **To cite this version:**

Siwar Cherbib, Ibtissem Jlalia, Taha Chabbah, Saber Chatti, Catherine Marestin, et al.. Design of New Partially Bio-Based Polyguanamines for the Reversible Adsorption of Phenolic Molecules from Olive Mill Wastes. *Chemistry Africa*, 2024, 7 (8), pp.4469-4479. 10.1007/s42250-024-01081-3 . hal-04780968

HAL Id: hal-04780968

<https://hal.science/hal-04780968v1>

Submitted on 13 Nov 2024

HAL is a multi-disciplinary open access archive for the deposit and dissemination of scientific research documents, whether they are published or not. The documents may come from teaching and research institutions in France or abroad, or from public or private research centers.

L'archive ouverte pluridisciplinaire **HAL**, est destinée au dépôt et à la diffusion de documents scientifiques de niveau recherche, publiés ou non, émanant des établissements d'enseignement et de recherche français ou étrangers, des laboratoires publics ou privés.

Design of new partially bio-based polyguanamines for the reversible adsorption of phenolic molecules from olive mill wastes

Siwar Cherbib^{1), 6)}, Ibtissem Jλία³⁾, TahaChabbah²⁾, Saber Chatti³⁾, Catherine Marestin²⁾, Regis Mercier²⁾, StefanWeidner⁴⁾, Herve Casabianca⁵⁾, Nicole Jaffrezic-Renault^{5) a)*}, Houyem Abderrazak¹⁾

- 1) National Institute of Research and Physicochemical Analysis(INRAP), LMU, Biotechnopole of Sidi Thabet, 2020 Ariana, Tunisia
- 2) University of Lyon, Institute of Polymer Materials, UMR 5223, 7, Avenue Jean Capelle, 69100Villeurbanne,France
- 3) National Institute of Research and Physicochemical Analysis(INRAP), LSN, Biotechnopole of Sidi Thabet, 2020 Ariana, Tunisia
- 4) Bundesanstalt für Materialforschung und prüfung (BAM) Fachbereich 6.3 “Strukturanalytik” Richard-Willstätter-Strasse 11, 12489 Berlin Germany
- 5) University of Lyon, Institute of Analytical Sciences, UMR 5280, 5 Rue de la Doua, 69100 Villeurbanne, France
- 6) University of Carthage, Faculty of Sciences, Zarzouna, 7021, Bizerte, Tunisia

*Corresponding author: e-mail: nicole.jaffrezic@univ-lyon1.fr

Abstract:

Olive mill wastewater produces a variety of potent antioxidants, including hydroxytyrosol, oleuropein, and tyrosol, that have been widely used in agriculture, pharmacy, and cosmetics. This study aims to design new poly(guanamine)s phases by polycondensation of modified triazine monomers with both petro-based and biosourced diamines, to act as stationary phases for the uptake of these phenolic molecules. The characterization of the obtained polymers was performed by NMR spectroscopy, differential scanning calorimetry (DSC) and thermogravimetric analysis (TGA). The adsorption results showed that the newly synthesized polymers can effectively uptake the less polar phenolic compounds, ferulic acid and caffeic acid. The isosorbide-based polymer (P6) presented the highest sorption efficiency, due to the hydrophilic properties of isosorbide associated with the proton affinity of the triazine groups. All the phenolic compounds were successfully desorbed from the P6 polymer using a minimal amount of a methanol/acetonitrile mixture. P6 polymer could be used for four successive adsorption processes without loss of efficiency.

Keywords: Olive mill wastewater, triazine groups, isosorbide, adsorption, phenolic compounds

a) New address : Université de Franche-Comté, UTINAM Institute, 25030 BESANCON, France

1. Introduction :

Olive mill wastewater (OMW) is a major by-product of the olive oil production process [1], which has always posed significant environmental and health problems. Produced mainly in Mediterranean countries, this effluent contains large quantities of organic matter, including phenolic compounds, fatty acids and other pollutants. Characterized by their strong odors, dark coloration and acidic pH (generally between 4 and 5) [2, 3], OMW are commonly discharged untreated into the environment, contributing to significant ecological degradation. This study explores the impact of OMW, highlights the beneficial properties of its phenolic components and proposes sustainable approaches for their management.

The traditional and industrial processes of extracting olive oil generate substantial volumes of olive mill wastewater (OMW), and it is common practice to discharge OMW into the natural environment without any treatment. This represents a problematic practice due to the high toxicity of the effluent [4], which can cause water and soil contamination [5], inhibiting plant growth, reducing soil fertility and killing aquatic life. OMW can contain more than 30 phenolic compounds [6]. The main ones are phenolic acids (such as vanillic, gallic, caffeic, and ferulic acids), phenolic alcohols (such as 3,4-dihydroxyphenyl ethanol, known as hydroxytyrosol, and p-hydroxyphenyl ethanol, known as tyrosol), flavonoids (such as luteolin and luteolin-7-glucoside), and secoiridoids (such as oleuropein and ligustroside) [7]. These Phenolic compounds have been listed by the United States Environmental Protection Agency (USEPA) and the European Union (EU) as priority pollutants due to their severe short- and long-term effects on human and animal health [8]. Additionally, the high content of phenolic compounds can be toxic to the microorganisms essential for ecosystem balance. The environmental impact is further aggravated by organic pollutants in effluents, which can increase biochemical oxygen demand (BOD) and chemical oxygen demand (COD) in water bodies, contributing to anoxia and serious disturbances in aquatic ecosystems."

Despite these challenges, the phenolic compounds present in OMW, such as hydroxytyrosol, tyrosol, oleuropein and others, when used within certain limits, are well known for their strong antioxidant properties [9]. These compounds are capable of scavenging free radicals, thereby reducing oxidative stress, a contributory factor in many chronic diseases, including cancer, cardiovascular disease and neurodegenerative disorders [10]. The antioxidant activity of these compounds has drawn attention to their potential applications in the agri-food, pharmaceutical and cosmetology sectors. For example, hydroxytyrosol, one of OMW's major

phenolic compounds, is used as a food supplement in a large selection of products such as dairy products, oils and fats, chocolates, beverages and so on. It is also able to reduce the risk of coronary heart disease and is an anti-inflammatory [11], and in cosmetics for protecting skin from environmental damage and aging. It also helps reduce inflammation [12], wrinkles, and other indications of skin aging [13], making it a perfect choice for anybody trying to improve their skin's appearance organically.

These beneficial properties of phenolic compounds have led to increased interest in the valorization of OMW. Recent research has focused on developing methods to extract these valuable compounds effectively and sustainably [14] which include liquid/liquid extraction [15], ultrasound-assisted extraction [16], microwave-Assisted Water Extraction [17] and adsorption [18]. Among these, adsorption is particularly noteworthy for its efficiency and environmental friendliness [19, 20]. This method does not generate secondary pollutants, which is a significant advantage over other techniques like oxidation, which can produce harmful byproducts. The development of technologies to recover and commercially use phenolic compounds not only minimizes environmental impact, but also adds economic value to the olive oil production process. This approach is in line with the principles of the circular economy, where waste is seen as a resource to be reused and reallocated wherever possible.

In recent years, many different adsorbents have been developed for the adsorption of phenolic compounds, such as silica gel [21], clay [22], carbonaceous materials [23, 24]. In this context, the idea is to design new chelating monomers and incorporate them into the polymer structure, which are able to adsorb the phenolic compounds from the OMW. From DFT studies, it was shown that for the adsorption of the bisphenols detected in OMW, on microporous resins occurred through hydrogen-bonding. The higher interaction energy was obtained for the carboxylic group, while the resin with amino groups presents the highest adsorption capacity [25]. The effect of the contain of amino groups in copolymer structures based on N-vinylimidazole on the adsorption of rutin was studied. Rutin adsorption process was found to be exothermic, the absolute value of ΔH increasing with the percentage of amino groups, and a spontaneous chemisorption process [26]. N-vinylimidazole monomer was used for the synthesis of hydroxytyrosol magnetic molecular imprinted polymer for the solid-phase extraction of hydroxytyrol from olive leaves [27]. Among the diverse heterocyclic structures, the triazine group was chosen because of its rigidity and stability under various conditions. In addition, since the triazine ring is a soft Lewis base and the nitrogen atoms can act effectively as hydrogen bond acceptors, as in N-vinylimidazole [28].

In this study, we aim to introduce modified triazine chloride groups into the structure of polyguanamines [29]. Polyguanamines can be synthesized via polycondensation reactions involving diamines and triazine derivatives [30]. By adjusting the types of diamines used and modifying the substituents on the triazines, we can tailor the resulting polyguanamines to exhibit specific properties such as solubility, thermal stability, and adsorption capacity.

Herein, two diamines were chosen to modify the 1,3,5-triazine groups, such as, two modified triazine dichloride monomers were selectively prepared by substituting one chloride ion of cyanuric chloride with diethylamine or diethanolamine. For the diamines, we selected two petro-based monomers: Bis[4-(4-aminophenoxy)phenyl]sulfone and 4,4'-(9H-fluorene-9,9-diyl)dianiline (diamine cardo), as well as a biosourced monomer: ((hexahydrofuro[3,2-b]furan-3,6-diyl)bis(oxy))dianiline (isosorbide). The choice of biosourced diamine based on isosorbide is motivated by the positive effect of incorporating this bio-based synthon into the polymer structure to enhance the adsorption of pollutants from water [31-33].

The six synthesized polyguanamines adsorbents were characterized using Nuclear Magnetic Resonance (NMR) spectroscopy, Gel Permeation Chromatography (GPC), Differential Scanning Calorimetry (DSC), and Thermogravimetric Analysis (TGA). The adsorption efficiency of the prepared polymers was then tested toward four target molecules (hydroxytyrosol, tyrosol, ferulic acid, and caffeic acid), as well as the re-extraction of the adsorbed phenolic compounds for their further use as antioxidants and the recyclability of the polymers.

2. Materials and methods:

2.1. Reagents and standards

Starting materials and solvents such as N,N-dimethylsulfoxide (DMSO) ($\geq 99.9\%$), tetrahydrofuran (THF) ($\geq 99.9\%$), N,N-dimethylformamide (DMF) ($\geq 99.9\%$), and other reagents were purchased from commercial sources and were used without any further purification. 1,4:3,6-dianhydro- D-glucitol (isosorbide) ($\geq 99\%$), cyanuric chloride (99%), fluoro-4-nitrobenzene ($\geq 99\%$), diethanolamine ($\geq 98\%$) and diethylamine ($\geq 99.5\%$) were purchased from Sigma Aldrich.

The following phenolic compounds with different functionality and polarity, were selected as target compounds: hydroxytyrosol, tyrosol, the more polar ones and caffeic acid, ferulic acid. They were purchased with purity higher than 99%. (See Figure 1 for molecule structures and polarity). The adsorption of these types of organic molecules is of great interest because of the difficulty of their extraction from water due to their high affinity with water (log Kow less

^{a)} New address : Université de Franche-Comté, UTINAM Institute, 25030 BESANCON, France

than 3.3). However, the polyamines were chosen for their reactivity (molecule capable of interacting by σ - π interactions (Halogen, N, O, P, S) or by H-X hydrogen bonding (X = O, N, S)).

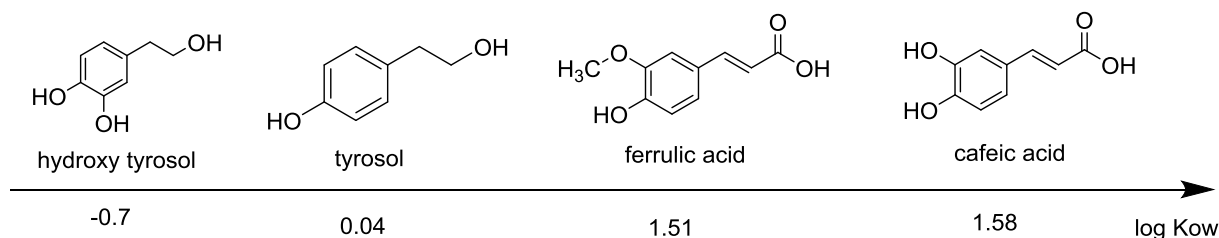


Figure 1: Chemical structure and polarity of phenolic compounds in olive oil waste

2.2. Characterization methods

^1H NMR spectra were recorded at 300 MHz at 25°C on a Brücker spectrometer using DMSO- d_6 as solvent. Chemical shifts were expressed in ppm relative to TMS.

The decomposition temperatures of the polymers were measured by thermogravimetric analysis (TGA) using a thermogravimetric analyzer type TGA Q50. The measurements were performed at a heating rate of 10°C/min in an inert atmosphere.

The glass transition temperatures were measured by differential scanning calorimetry (DSC) using a DSC 822e Mettler Toledo calorimeter. These measurements were performed under nitrogen, as a sweep gas, with a flow rate of 50 mL/min and with a heating rate of 10°C / min. Furthermore, they were characterized by size exclusion chromatography (SEC) and Gel Permeation Chromatography (GPC).

2.3. Monomer synthesis

Synthesis of the bio-based diamine: 4,4'-((hexahydrofuro[3,2-b]furan-3,6-diyl)bis(oxy))dianiline (1b):

The synthesis of the monomer from isosorbide can be summarized in two steps (Figure 2)

Step1: Synthesis of 3,6-bis(4-nitrophenoxy)hexahydrofuro[3,2-b]furan (1a): Isosorbide (10.00 g) was dissolved in DMSO (125 mL), then fluoronitrobenzene (15.9 mL) and K_2CO_3 (20.82g) were added. The mixture was heated to 110°C under N_2 atmosphere and stirring. After 24h of reaction time and cooling, the suspension was filtered and then vacuum dried at 60°C.

Step2: Synthesis of 4,4'-((hexahydrofuro[3,2-b]furan-3,6-diyl)bis(oxy))dianiline (1b): The intermediate 1a (10.00g) was dissolved in THF (20.0 mL). A mixture of hydrazine (6.70 mL)

and THF (17.0 mL) was added drop by drop to the solution at room temperature under agitation. Then, 10% of palladium on charcoal was added. The solution was agitated at room temperature and then heated to 40°C for 24 h. Afterward, the solution was washed simultaneously with THF, filtered and then vacuum dried.

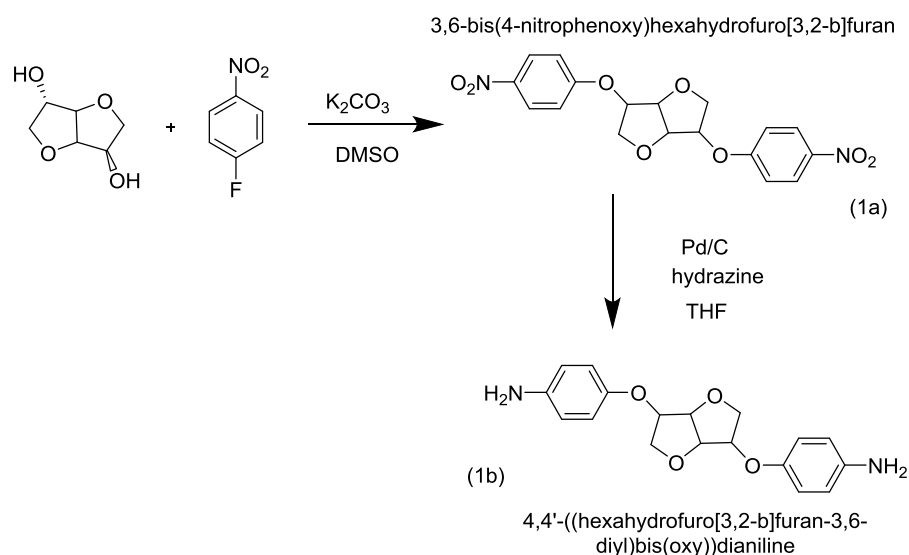


Figure 2: Synthesis of 4,4'-((hexahydrofuro[3,2-b]furan-3,6-diyl)bis(oxy))dianiline (**1b**)

During each step, the intermediates were characterized by 1H NMR in $CDCl_3$ and $DMSO-d_6$. Figures S1 and S2 respectively show the NMR spectra of monomers (1a) and (1b). The chemical structure of the intermediate (1a) was confirmed by analyzing its 1H NMR spectrum, as depicted in Figure S1.

1H NMR (300 MHz, $CDCl_3$): δ (ppm): 4.20-4.03 (m, 4H); 4.65 (d, $J=6Hz$, 1H); 4.91-4.85 (m, 2H); 5.06 (t, $J=6Hz$, 1H); 7.07-7 (m, 4H) and 7.65-7.60 (m, 4H).

In the NMR spectrum of monomer (1b) (Figure S2), the same peaks as those for monomer (1a) are observed, but with the proton (NH_2) appearing around 3.68 and 3.88 ppm.

1H NMR (300 MHz, $DMSO-d_6$): δ (ppm): 4.1-3.65 (m, 4H); 4.50 (d, $J=3Hz$, 1H); 4.67-4.62 (m, 6H); 4.8 (t, $J=3Hz$, 1H); 6.54-6.48 (m, 4H) and 6.74-6.66 (m, 4H).

Synthesis of monomers from Cyanuric chloride

Cyanuric Chloride (9.220 g) was dissolved in acetone (50.0 mL); (diethanolamine (5.250 g, to synthesis 2a)/ diethylamine (5.000g, to synthesis 2b) and K_2CO_3 (5.050 g) were added dropwise into the solution at low temperature under hustle. After 3 h, the suspension was filtered and finally dried in vacuum overnight at 60°C. The yields of 2a and 2b are 76% and 85%, respectively.

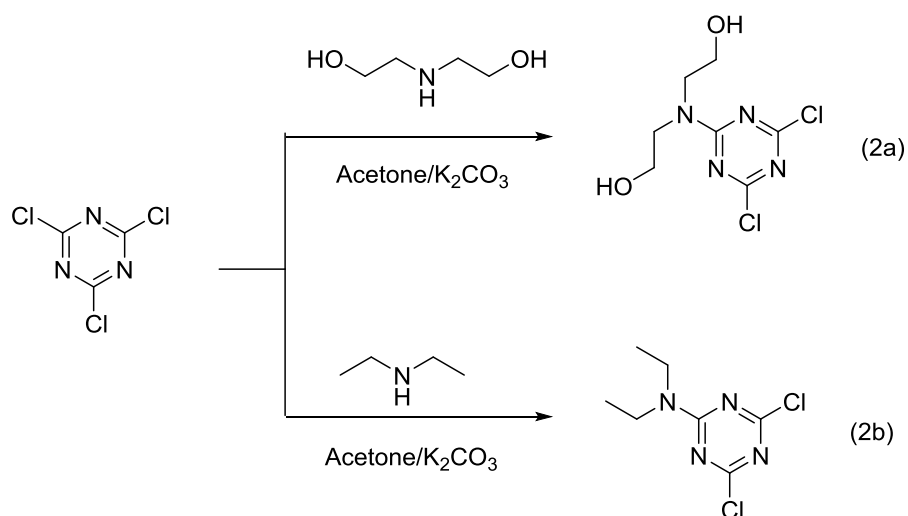


Figure 3: Synthesis of monomers (2a) and (2b)

The ^1H NMR spectrum of monomer (2a) presented in Figure S3 confirms its structure with the presence of the proton Ha pic at 3.60 ppm, a triplet at 3.68 ppm corresponding to the Hb proton and a peak at 3.46 ppm corresponding to the Hc proton.

The ^1H NMR spectrum of monomer 2b (Figure S4) exhibits all the protons characteristic of Hb at 3.58 ppm and a tripled at 1.15 ppm corresponding to the Ha proton.

1.1. Synthesis of the polymers

All polymers were synthesized in only one step through the polycondensation of cyanuric chloride modified monomers (2a/2b) with three different monomers (Bis[4-(4-aminophenoxy)phenyl]sulfone (1d) / 4,4'-(9H-fluorene-9,9-diyl)dianilines (1c)/ 4,4'-((hexahydrofuro[3,2-b]furan-3,6-diyl)bis(oxy))dianiline (1b) to obtain 6 polymers (P1– P6). It is an aromatic nucleophilic substitution carried out in a polar aprotic solvent, dimethylformamide (DMF, 20% solid). The polymerization reactions were catalyzed by K_2CO_3 and heated for 24 hours. Finally, the mixture was poured into water and then the obtained polymer was collected by filtration, and dried under vacuum at 80°C .

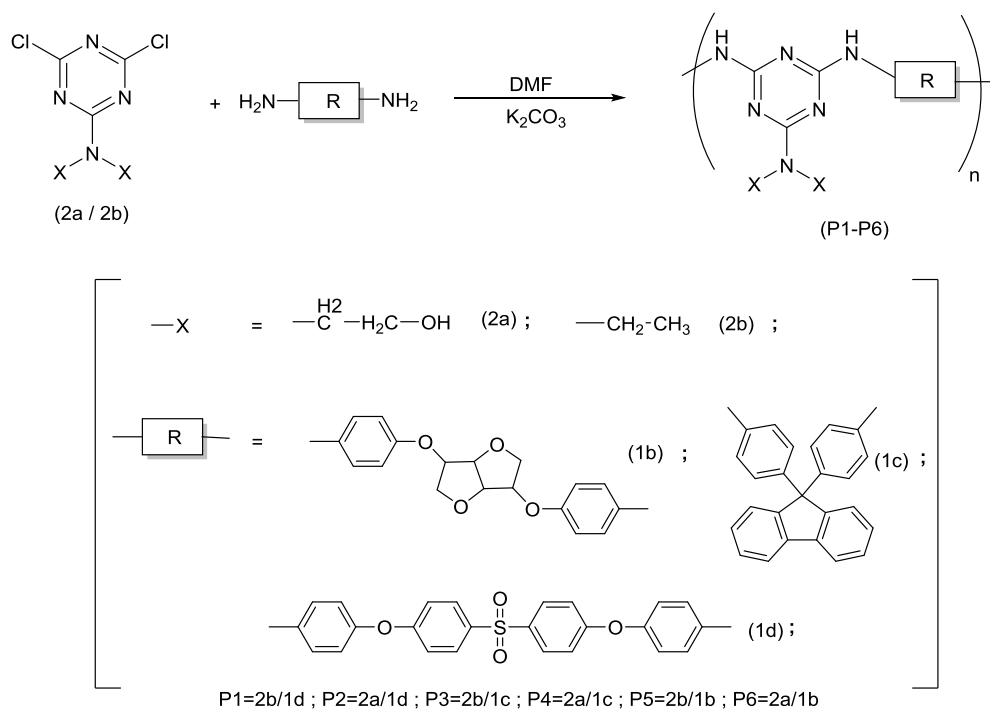


Figure 4: The synthetic routes of the poly(polyguanamine)s polymers P1–P6 (P1=2b/1d ; P2=2a/1d ; P3=2b/1c ; P4=2a/1c ; P5=2b/1b ; P6=2a/1b)

1.2. Adsorption experiments on the polymers P1-P6

To achieve a similar surface for all developed polymers, 500 mg of each polymer were dissolved in 9.50 mL of DMF to reach a concentration solution equal to 5 w/w % and then precipitated into 400 mL of deionized water and agitated for 15 min. A very fine powder was extracted after filtration.

Adsorption tests were carried out in 10.0 mL scintillation flasks, stirred magnetically, in a room under air conditioning at $25 \pm 1^\circ\text{C}$. Into these flasks, a mass of 60.0 mg of ground polymer with the addition of 3.000 g of sodium chloride (NaCl) were introduced, then 10.0 mL of target phenolic compounds were added concentration: 5 mg/L and pH=2). The mixture was placed on a stirring plate with a speed of 900 rpm and after each time period, a volume of 1 mL of the solution was collected via a syringe and then filtered through a $0.45 \mu\text{m}$ PTFE membrane filter. The final concentration of the phenolic compound was measured by High Performance Liquid Chromatography (HPLC) equipped with an Agilent XDB C18 column ($4.6 \text{ mm} * 100 \text{ mm} * 1.8 \mu\text{m}$) at an oven temperature of 50°C . The measurements were performed at the wavelength of 245 nm. The mobile phase consisted of 0.1 % (v/v) of orthophosphoric acid in water (eluent A) and of acetonitrile (eluent B). The flow rate was set to 1 mL/ min. The injection volume for all samples was adjusted to 10 μL .

The adsorption efficiency (%) of the pollutants by the polymers was calculated following equation 1:

$$\text{Adsorption efficiency} = 100 * ((C_i - C_t) / C_i) \quad \text{Eq. 1}$$

Where:

C_i : initial concentration

C_t : the concentration of pollutant at time t (mmolL^{-1})

1.3. Regeneration of the adsorbent

The regeneration experiments were performed by a series of successive extractions. After adsorption, the desorption process of the phenolic compound was carried out using 10.0 mL of methanol/acetonitrile (50/50) as a washing solvent for 40 min. Finally, the polymer was recovered by filtration, washed with deionized water and dried for reuse in the next cycle.

2. Results and discussion

2.1. Synthesis and characterization of polymers P1–P6

In order to prepare the polyguanamines polymers, we first synthesized two 2-substituted 4,6-dichloro 1,3,5-triazine monomers, (2a) and (2b), from cyanuric chloride with ethanolamine and ethylamine, respectively, in acetone in the presence of K_2CO_3 as HCl scavenger (Figure 3). The structure of these two triazine containing monomers were characterized using NMR spectroscopy, revealing that they had purities adequate for polycondensation reaction.

A series of polyguanamines polymers were prepared through conventional solution polycondensation of the synthesized monomers (2a) and (3a) with three diamines : (4,4'-((hexahydrofuro[3,2-b]furan-3,6-diyl)bis(oxy))dianiline; 2,2-((4,6-dichloro-1,3,5-triazin-2-yl)azanediyl)bis(ethan-1-ol) and 4,6-dichloro-N,N-diethyl-1,3,5-triazin-2-amine) in polar aprotic solvent (DMF, 20% cc) in the presence of potassium carbonate (as catalyst and HCl acceptor), at 160 °C for 24 h (Figure 4). The results of the polymerization are summarized in Table 1.

During the polymerization of the dichloro monomer (2b) with the diamine cardo (1c) precipitation were observed due to the low solubility of the condensation product.

Table 1: Physico-chemical properties of the resulting polymers P1-P6

Ref.	Monomers	Yields	T _{5%}	T _g (°C)	M _n	M _w	PD ^(d)
------	----------	--------	-----------------	---------------------	----------------	----------------	-------------------

^{a)} New address : Université de Franche-Comté, UTINAM Institute, 25030 BESANCON, France

Polymer		(%)^(a)	(°C)^(b)	(c)	(Da)^(d)	(Da)^(d)	
P1	2b/1d	74	203	100	8663	14752	1.70
P2	2a/1d	95	217	102	4828	14967	3.1
P3	2b/1c	NS*	-	-	NS	NS	-
P4	2a/1c	92	229	112	4663	13058	2.8
P5	2b/1b	85	242	130	6940	15200	2.19
P6	2a/1b	82	373	142	3720	12351	3.32

*NS: insoluble

a) Precipitation into water and washing with methanol, evaporation under a vacuum at 80 °C.

b) T_{5%}: Temperature of 5 % weight loss, determined by TGA at 10 °Cmin⁻¹ heating rate under nitrogen gaz.

c) Obtained by DSC with a heating rate of 10 °C/min.

d) Number and weight-averaged molecular weights and polydispersity (PD) determined by GPC in CHCl₃ against polystyrene standards

As shown in Table 1, the five soluble polyguanamines were obtained with good yields in the range of 74–95%. The average molecular weight (M_n) of the synthesized polymers, determined by gel permeation chromatography, is between 3720 and 8663 g/mol and the dispersity index range from 1.7 to 2.3. The chemical structure of the resulting polyguanamines were ascertained by ¹H NMR analysis. A detailed description of the NMR data recorded from P1, P2, P4- P6 are given in Figure S5-S9.

The presence of characteristic peaks for each polymer in the ¹H NMR spectra depicted in figures S5-S9 supports the structural integrity of the synthesized polymers (P1-P6)

The thermal properties of the synthesized polymers were determined by differential scanning calorimetry (DSC) and Thermogravimetric analysis (TGA). The results of these analyses are presented in Table 1 and the TGA and DSC diagrams of the polymers P1, P2, P4- P6 are represented in Figure 5 and 6, respectively.

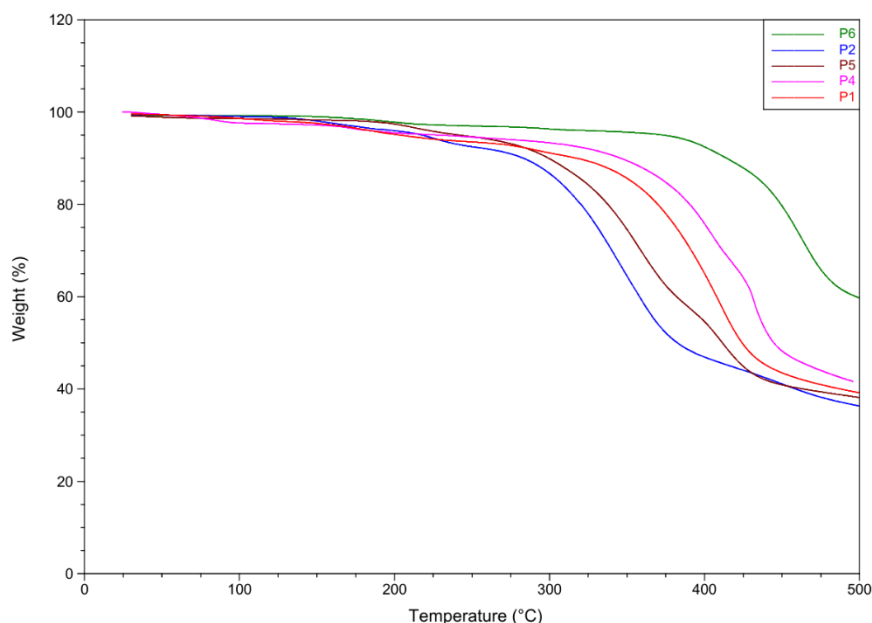


Figure 5: TGA curves of the polymers from P1 to P6

The thermal stability of the synthesized polymers was determined by thermogravimetry from 25 °C to 500 °C at a heating rate of 10 °C/min under nitrogen atmosphere. As it can be concluded from the overall data in Table 1, the decomposition onset temperature that corresponds to 5% weight loss for all polymers is ranging from 203 to 373 °C. The P6 polymer admits the higher temperature of T5% which is often associated with a better resistance at high temperatures.

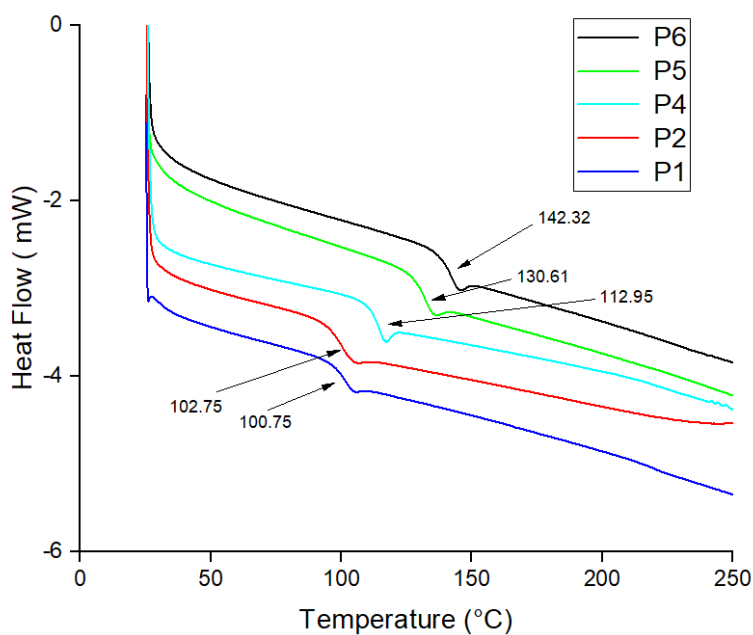


Figure 6: DSC curves for polymers from P1 to P6

However, the presence of a single inflection point in the DSC thermogram (figure 6), corresponding to the glass transition temperature (T_g), indicates their amorphous character. It can be concluded that the biobased polymers (P5 and P6) present the highest glass transition temperature ($T_g = 142^\circ\text{C}$ for P6 and $T_g = 130^\circ\text{C}$ for P5) compared to the other polymers (Table 1), for instance, this temperature is merely 102°C for P2. The P5 and P6 polymers with high T_g tend to be stiffer and retain their dimensions at higher temperatures, which also means they can withstand attack by aggressive chemicals without suffering significant degradation, as previous work [34, 35] has revealed due to the high rigidity promoted by the combined presence of triazine and isosorbide. The stronger hydrogen bonds and intermolecular forces that the P6 polymer can undergo may also enhance the value of the T_g .

2.2 Adsorption behavior of the polymers

The adsorption phenomenon in our case is a physical adsorption, based only on a physical or non-covalent interaction between the polymer and the phenolic compounds, which took place on the surface of the adsorbing particles. In fact, many interactions are susceptible to occur, such as π - π interactions, hydrophobic interactions, weak Vander Waals interactions as well as H-bonds. In this part of the work, we evaluated the adsorption efficiency of the four phenolic compounds (Figure 1) on the synthesized polymers P1, P2 P4-P6. The adsorption process of these polymers was observed after different periods of time (1, 3 and 24 h), as described in the experimental section. The adsorption efficiency of the different polymers is summarized in Table 2.

Table 2: Adsorption efficiency (%) of the target aromatic molecules on P1-P6 polymers after different periods.

Polymer	P1			P2			P4			P5			P6		
	1	3	24	1	3	24	1	3	24	1	3	24	1	3	24
Hydroxytyrosol	18	22	24	15	20	28	20	25	40	23	26	35	73	77	78
Tyrosol	19	24	27	17	28	53	25	39	68	22	27	34	84	86	88
Caffeic Acid	49	63	68	31	58	80	33	62	93	59	80	89	93	95	96
Ferulic Acid	62	77	84	50	71	92	43	69	97	62	81	87	100	100	100

The results show that the adsorption efficiency increases significantly after 1 h of contact until reaching almost 100% after 24 h. It can be noticed that the less polar molecules have a small tendency to be adsorbed, compared to the more polar ones. For example, it can be clearly seen that after 24 hours of contact with polymer P1 (hydrophobic polymer), only 24 % of hydroxy

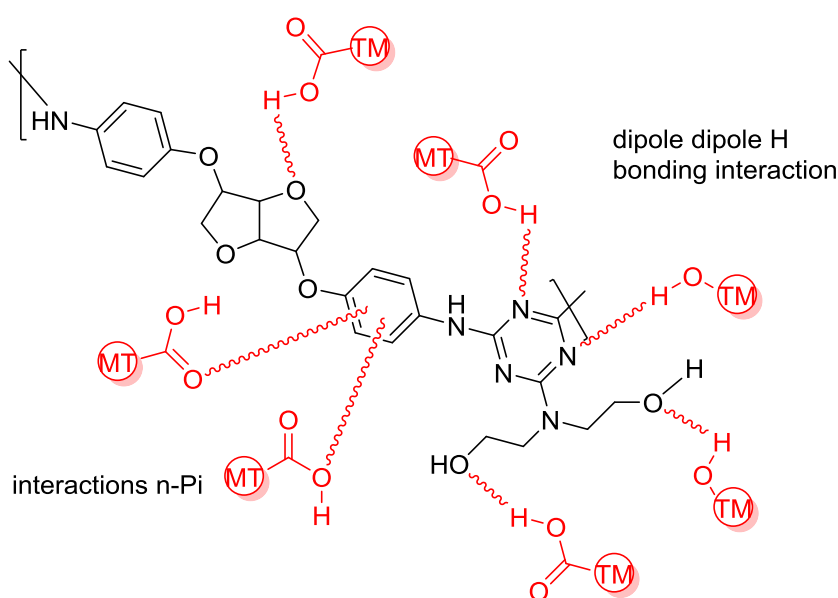
tyrosol ($\log K_{ow} = -0.7$) was adsorbed while 84 % of caffeic Acid ($\log K_{ow} = 1.58$) was adsorbed.

Recently, several research studies have reported on the multi-step preparation of a series of semi-aromatic polymers derived from isosorbide diol, demonstrating high adsorption efficiency for organic micropollutants [34, 35]. Based on these findings, the results of the bio-based polymers P5 and P6 compared to the Petro-based polymers (P1, P2 and P4) in this work, confirm the positive effect of incorporating isosorbide into the polymer structure. This can be explained by the special structure and chirality of Isosorbide unit associated with the complexing proprieties of the triazine unit that make these bio-based polymers much more hydrophilic which increases their tendency to attract the organic compounds.

On the other hand, we comparing the adsorption results of P5 and P6, it can be shown that the presence of the hydroxyl (OH) group in the polymer structure (P6) increases the sorption of hydroxytyrosol and tyrosol through H-bonding. It was found that the efficiency of adsorption of hydroxytyrosol (the most polar molecule) increased from 35% to 78% (compared to the polymer P5).

WE compared the adsorption results of our polymer P6 with those of a polymer studied by Brirmi et al. [36] and found that the adsorption efficiency of phenolic compounds was similar for durations of 3, 5, and 24 hours, but higher for a one-hour treatment. This indicates that our phases have a faster adsorption rate.

A general mechanism of adsorption of the different target molecules is proposed in Figure 7.



TM = Target molecules

Figure 7: Proposed adsorption mechanism of target molecules on the polymer P6

The adsorption mechanism for polyphenols is based on non-covalent interactions between the polymer and the target molecules. In fact, numerous interactions are likely to occur, such as $n-\pi$ interactions, hydrophobic interactions and H-bonds [37]. The incorporation of the hydroxyl group into the triazine chemical structure can form an attractive polar cavity for trapping hydrophilic polyphenols. In addition, triazine nitrogen atoms can act as hydrogen bond acceptors (figure 7). Moreover, the adsorption of polar molecules is also favored by the hydrophilicity of isosorbide moieties. Also, the strong polarizing effect of the oxygen atom in the target molecule defines a strong $n\rightarrow\pi^*$ interaction on the aromatic rings.

2.2. Desorption of phenolic compounds:

Recovery of phenolic compounds (hydroxytyrosol and tyrosol) and sorbent regeneration are important steps for cost-effective extraction of the target molecules. Consequently, a study of the number of regeneration cycles (adsorption-desorption) is crucial. In this part, the regeneration of the P6 polymer was studied, P6 being the most efficient polymer, capable of adsorbing the maximum number of target molecules. A series of desorption experiments were performed using a washing solution mixture of methanol/acetonitrile (50/50) chosen for its polarity and ability to dissolve phenolic molecules. The desorption was then realized with 3 mL of the washing solution at room temperature. The removal efficiency on the P6 polymer for the target molecules relative to the different times, is presented in Table 3. Different desorption times (10, 20, 40 and 60 min) were tested; as it can be concluded from the reported results the quantity of desorbed analyte did not increase after 40 min.

Table 3: Desorption rate of benzene derivatives from P6 polymer by Methanol/Acetonitrile mixture (50/50) after different durations

Time (minutes)	10	20	40	60
Solvent	Meth/Acn* 50/50	Meth/Acn* 50/50	Meth/Acn* 50/50	Meth/Acn* 50/50
Target molecules	Desorption (%)			
Hydroxytyrosol	24	33	72	75
Tyrosol	29	41	77	78
Caffeic Acid	36	62	78	79
Ferulic Acid	45	66	81	83

Desorption efficiency (%) was determined as the desorbed quantity of the acetonitrile/methanol mixture relative to the pre-adsorbed quantity. As shown in Table 3, the highest percentages of desorption were in the range of 72 to 81% after 40 min of contact.

After optimization of the desorption rate by methanol/acetonitrile mixture (50/50), the reusability of the P6 polymer was studied, through five successive adsorption/desorption cycles, under optimized conditions (after 60 min of contact with the target molecules and desorption by equilibration with 10 mL of methanol/acetonitrile mixture (50/50) for 40 min). The results are listed in Table 5.

Table 4: Adsorption/desorption cycles obtained with the P6 polymer

Cycle number	C1	C2	C3	C4	C5
Target molecules					
hydroxytyrosol	73	71	68	65	52
Tyrosol	84	81	79	75	64
Caffeic Acid	93	86	78	75	69
Ferrulic Acid	100	98	95	86	78

According to Table 4, it can be noted that the polymer P6 shows good reusability after 4 cycles. The adsorption rate decreased by 14% for the less polar compounds while it decreases by 8% for the most polar ones.

3. Conclusion :

In the present work, we successfully synthesized five polyguanamines polymers containing triazine groups. These polymers were characterized by NMR spectroscopy, exclusion chromatography (SEC), gel permeation chromatography (GPC), TGA and DSC analysis. All the polymers were synthesized in a one-step reaction and subsequently tested as solid phase adsorbent for phenolic compounds present in olive oil wastes. Sorption results showed that the biobased polymer P6 presents better adsorption efficiency for all tested phenolic compounds compared to petroleum-based polymers. We also concluded that the incorporation of the triazine group in the chemical structure of polymers has a major effect on the increase of the adsorption efficiency. Four consecutive adsorption/desorption cycles of the four phenolic compounds were shown to be effective for optimal use of the P6 polymer for the adsorption and the recovery of the phenolic compounds such as hydroxytyrosol and tyrosol.

Acknowledgments

The research leading to these has received funding from the European Union Horizon 2020(TUNTWIN) research and innovation program under grant agreement n° 952306.

We would like to acknowledge the financial support of CAMPUS-FRANCE and the French Embassy in Tunisia for the SSHN grant, of the POLYAM project, of the High Ministry of Education and Research in Tunisia for doctoral grant as well as University of Carthage for financial support. Region Auvergne Rhone Alpes is acknowledged for the Pack Ambition International Project, EMBAI #246413 and CNRS for the International Research Project NARES.

REFERENCES

1. El Kafz G, Cherkaoui E, Benradi F, Khamar M, Nounah A (2023) Characterization of Two Olive Mill Wastewater and Its Effect on Fenugreek (*Trigonella foenum-graecum*) Germination and Seedling Growth. *J Ecol Eng.* <https://doi.org/10.12911/22998993/171545>
2. Saouini HE, Bouzid S, Trankil A, Amharref M, Bernoussi AS (2023) Application of Statistical Methods for the Comparative Study of the Degree of Pollution of Wastewater Collected from Three Olive Mills in Tangier-Tetouan-Al Hoceima Region (Northern Morocco). *J Ecol Eng.* <https://doi.org/10.12911/22998993/160684>
3. Shabir S, Ilyas N, Saeed M, Bibi F, Sayyed RZ, Almalki WH (2023) Treatment technologies for olive mill wastewater with impacts on plants. *Environ Res.* <https://doi.org/10.1016/j.envres.2022.114399>
4. Fleyfel LM, Leitner NKV, Deborde M, Matta J, El Najjar NH (2022) Olive oil liquid wastes—Characteristics and treatments: A literature review. *Process Saf Environ.* <https://doi.org/10.1016/j.psep.2022.10.035>
5. Kovačević M, Stjepanović N, Trigui S, Hackenberger DK, Lončarić Z, Glavaš OJ, Kallel A, Hackenberger BK (2022) Assessment of adverse effects of olive mill waste water and olive mill waste contaminated soil on springtail *Folsomia candida*. *Chemosphere.* <https://doi.org/10.1016/j.chemosphere.2022.134651>
6. Foti P, Romeo FV, Russo N, Pino A, Vaccalluzzo A, Caggia C, Randazzo CL (2021) Olive Mill Wastewater as Renewable Raw Materials to Generate High Added-Value Ingredients for Agro-Food Industries. *Appl Sci.* <https://doi.org/10.3390/app11167511>
7. Llorente DR, Gutiérrez DM, Rodríguez PS, Navarro P, Torrellas SA, García J, Larriba M (2023) Sustainable recovery of phenolic antioxidants from real olive vegetation water with natural hydrophobic eutectic solvents and terpenoids. *Environ Res J.* <https://doi.org/10.1016/j.envres.2022.115207>
8. Ben Othman F, Fadhel A, Balghouthi M (2022) Sustainable olive-oil mill wastewater treatment by distillation using a parabolic trough solar collector. *J. Water Process Eng.* <https://doi.org/10.1016/j.jwpe.2022.102947>

9. Kim HH, Jeong SH, Park MY, Bhosale PB, Abusaliya A, Kim HW, Seong JK, Ahn M, Park K, Gon Sup Kim (2023) Antioxidant effects of phenolic compounds in through the distillation of *Lonicera japonica* & *Chenpi* extract and anti-inflammation on skin keratinocyte. *Sci Rep*. <https://doi.org/10.1038/s41598-023-48170-w>
10. Rahman M, Rahaman S, Islam R, Rahman F, Mithi FM, Alqahtani T, Almikhlaifi MA, Alghamdi SQ, Alruwaili AS, Hossain S, Ahmed M, Das R, Emran TB, Uddin S (2022) Role of Phenolic Compounds in Human Disease: Current Knowledge and Future Prospects. *Molecules*. <https://doi.org/10.3390/molecules27010233>
11. Albuquerque BR, Heleno SA, Oliveira MBPP, Barros L, Ferreira ICFR (2020) Phenolic compounds: current industrial applications, limitations and future challenges. *Food Funct*. <https://doi.org/10.1039/D0FO02324H>
12. Serra M, Casas A, Teixeira JA, Barros AN (2023) Revealing the Beauty Potential of Grape Stems: Harnessing Phenolic Compounds for Cosmetics. *Int J Mol Sci*. <https://doi.org/10.3390/ijms241411751>
13. Kalasariya HS, Patel AK, Suthar R J, Pereira L (2023) Exploring the Skin Cosmetic Benefits of Phenolic Compounds and Pigments from Marine Macroalgae: A Novel Green Approach for Sustainable Beauty Solutions. *Preprints*. <https://doi.org/10.20944/preprints202307.0739.v1>
14. Alara OR, NH, Ukaegbu CI (2021) Extraction of phenolic compounds: A review. *Curr Res Food Sci*. <https://doi.org/10.1016/j.crfs.2021.03.011>
15. Azzam MOJ, Hazaimh SA (2021) Olive mill wastewater treatment and valorization by extraction/concentration of hydroxytyrosol and other natural phenols. *Process Saf Environ*. <https://doi.org/10.1016/j.psep.2020.10.030>
16. Cruz IG, Contreras MdM, Romero I, Castro E (2021) Sequential Extraction of Hydroxytyrosol, Mannitol and Triterpenic Acids Using a Green Optimized Procedure Based on Ultrasound. *Antioxidants*. <https://doi.org/10.3390/antiox10111781>
17. Cruz IG, Contreras MdM, Romero I, Castro E (2022) Optimization of Microwave-Assisted Water Extraction to Obtain High Value-Added Compounds from Exhausted Olive Pomace in a Biorefinery Context. *Foods*. <https://doi.org/10.3390/foods11142002>
18. Cabezas MC, Arévalo CMS, Roca JAM, Vela MCV, Blanco SA (2022) Recovery of phenolic compounds from olive oil washing wastewater by adsorption/desorption process. *Sep Purif Technol*. <https://doi.org/10.1016/j.seppur.2022.121562>
19. Li N, Fang J, Jiang P, Li C, Kang H, Wang W (2022) Adsorption Properties and Mechanism of Attapulgit to Graphene Oxide in Aqueous Solution. *Int J Environ Res Public Health*. <https://doi.org/10.3390/ijerph19052793>
20. Benaddi R, Osmane R, Zidan K, El Harfi K, Ouazzani N (2023) A Review on Processes for Olive Mill Waste Water Treatment. *Ecol Eng Environ Technol*. <https://doi.org/10.12912/27197050/169876>
21. Nayl AA, Abd-Elhamid AI, Aly AA, Bräse S (2022) Recent progress in the applications of silicabased nanoparticles. <https://doi.org/10.1039/D2RA01587K>
22. Chaari I, Touil A, Medhioub M (2021) Adsorption-desorption of phenolic compounds from olive mills wastewater using Tunisian natural clay. *Chin J Chem Eng*. <https://doi.org/10.1016/j.cjche.2020.12.020>
23. Kuśmierk K, Świątkowsk A (2023) Adsorption of Phenols on Carbonaceous Materials of Various Origins but of Similar Specific Surface Areas. *Separations*. <https://doi.org/10.3390/separations10080422>
24. Abid N, Masmoudi MA, Megdiche M, Barakat A, Ellouze M, Chamkha M, Ksibi M, Sayadi S (2022) Biochar from olive mill solid waste as an eco-friendly adsorbent for

- the removal of polyphenols from olive mill wastewater. *Chem Eng Res Des.* <https://doi.org/10.1016/j.cherd.2022.02.029>
25. Gou J, Zhang W, Wang XF, Hao D, Shen H, You N, Long WY (2023) Amino-carboxyl cellulose for adsorption of Cd²⁺ and Pb²⁺. *Chemosphere.* <https://doi.org/10.1016/j.chemosphere.2023.139705>
 26. Sahin S, Emik S, Kurtulbas M, Erdem M, Vasseghian Y (2022) Adsorption of rutin from olive mill wastewater using copolymeric hydrogels based on N-vinylimidazole: kinetic, equilibrium, and thermodynamics assessments. *Environ Res.* <https://doi.org/10.1016/j.envres.2022.113306>
 27. Yu Q, Gan H, Feng N, Li Y, Han Y (2021) Hydroxytyrosol magnetic molecularly imprinted polymers as sorbent for solid-phase extraction for selective recognition of hydroxytyrosol from Chinese olive leaves. *Mater Today Commun.* <https://doi.org/10.1016/j.mtcomm.2021.102992>
 28. Kenny PW (2022) Hydrogen-Bond Donors in Drug Design. *J Med Chem.* <https://doi.org/10.1021/acs.jmedchem.2c01147>
 29. Aldalbahi A, AlOtaibi BS, Thamer BM, El-Faham A (2022) Synthesis of New S-Triazine Bishydrazino and BishydrazidoBased Polymers and Their Application in Flame-Retardant Polypropylene Composites. *Polymers.* <https://doi.org/10.3390/polym14040784>
 30. Shibasaki Y, Koizumi T, Oishi Y (2023) Synthesis of High Refractive Linear to Branched Polyguanamines from 2-Amino-4,6-dichloro-1,3,5- triazine with Aromatic Diamines. *J Photopolym Sci Tec.* <https://doi.org/10.2494/photopolymer.36.385>
 31. Chabbah T, Abderrazak H, Souissi R, Martin PS, Casabianca H, Chatti S, Mercier R, Rassas I, Errachid A, Hammami M, Renault N (2020) A sensitive impedimetric sensor based on biosourced polyphosphine films for the detection of lead ions. *Chemosensors.* <https://doi.org/10.3390/chemosensors8020034>
 32. Chabbah T, Chatti S, Zouaoui F, Jlalía I, Gaiji H, Abderrazak H, Casabianca H, Mercier R, Weidner SM, Errachid A, Marestin C, Renault NJ (2022) New poly (ether-phosphoramidate)s sulfides based on green resources as sensitive films for the specific impedimetric detection of nickel ions. *Talanta.* <https://doi.org/10.1016/j.talanta.2022.123550>
 33. Jlalía I, Chabbah T, Chatti S, Schiets F, Casabianca H, Marestin C, Mercier R, Weidner SM, Kricheldorf HR, Errachid A, Vulliet E, Hammami M, Jaffrezic-Renault N (2022) Alternating bio-based pyridinic copolymers modified with hydrophilic and hydrophobic spacers as sorbents of aromatic pollutants. *Polym Adv Technol.* <https://doi.org/10.1002/pat.5578>
 34. Gomri M, Abderrazak H, Chabbah T, Souissi R, Martin PS, Casabianca H, Chatti S, Mercier R, Errachid A, Hammami M, Renault NJ (2020) Adsorption characteristics of aromatic pollutants and their halogenated derivatives on bio-based poly (ether-pyridine)s. *J Environ Chem Eng.* <https://doi.org/10.1016/j.jece.2020.104333>
 35. Chabbah T, Abderrazak H, Saint Martin P, Casabianca H, Kricheldorf HR, Chatti S (2020) Synthesis of Glux based polymers for removal of benzene derivatives and pesticides from water. *Polym Adv Technol.* <https://doi.org/10.1002/pat.5578>
 36. Birimi NEH, Chabbah T, Chatti S, Schiets F, Casabianca H, Marestin C, Mercier R, Weidner SM, Errachid A, Renault NJ, Ben Romdhane H (2022) Effect of the pendent groups on biobased polymers, obtained from click chemistry suitable, for the adsorption of organic pollutants from water. *Polym Adv Technol.* <https://doi.org/10.1002/pat.5809>
 37. Ghorbali R, Sellaoui L, Ghalla H, Petriciolet AB, Valencia RT, Barroso AS, Deng S, Ben Lamine A (2024) In-depth study of adsorption mechanisms and interactions in

the removal of pharmaceutical contaminants via activated carbon: a physicochemical analysis. Environ Sci Pollut Res. <https://doi.org/10.1007/s11356-024-33806-9>

Supplementary Material

Optimization of the design of partially biobased polymers with triazine groups for the reversible adsorption of phenolic molecules from olive mill wastes

Siwar Cherbib^{1),6)}, Ibtissem Jλία³⁾, Taha Chabbah²⁾, Saber Chatti³⁾, Catherine Marestin²⁾, Regis Mercier²⁾, Stefen Weidner⁴⁾, Nicole Jaffrezic-Renault^{5)*}, Houyem Abderrazak¹⁾

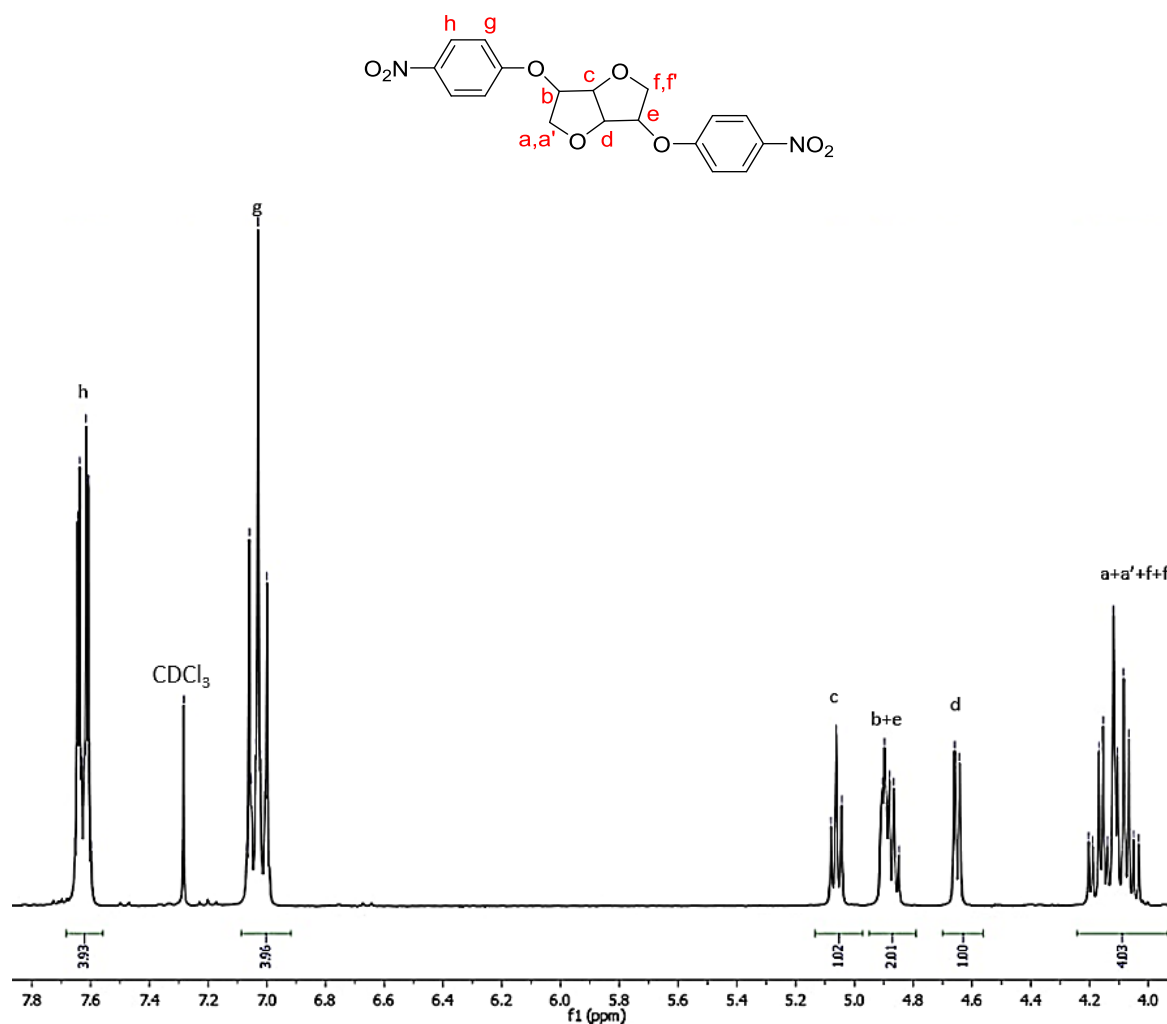


Figure S1. ¹H NMR spectrum of monomer 1a

¹H NMR (300 MHz, CDCl₃): δ (ppm): 4.20-4.03 (m, 4H); 4.65 (d, *J* = 6 Hz, 1H); 4.91-4.85 (m, 2H); 5.06 (t, *J* = 6 Hz, 1H); 7.07-7.00 (m, 4H) and 7.65-7.60 (m, 4H).

a) New address : Université de Franche-Comté, UTINAM Institute, 25030 BESANCON, France

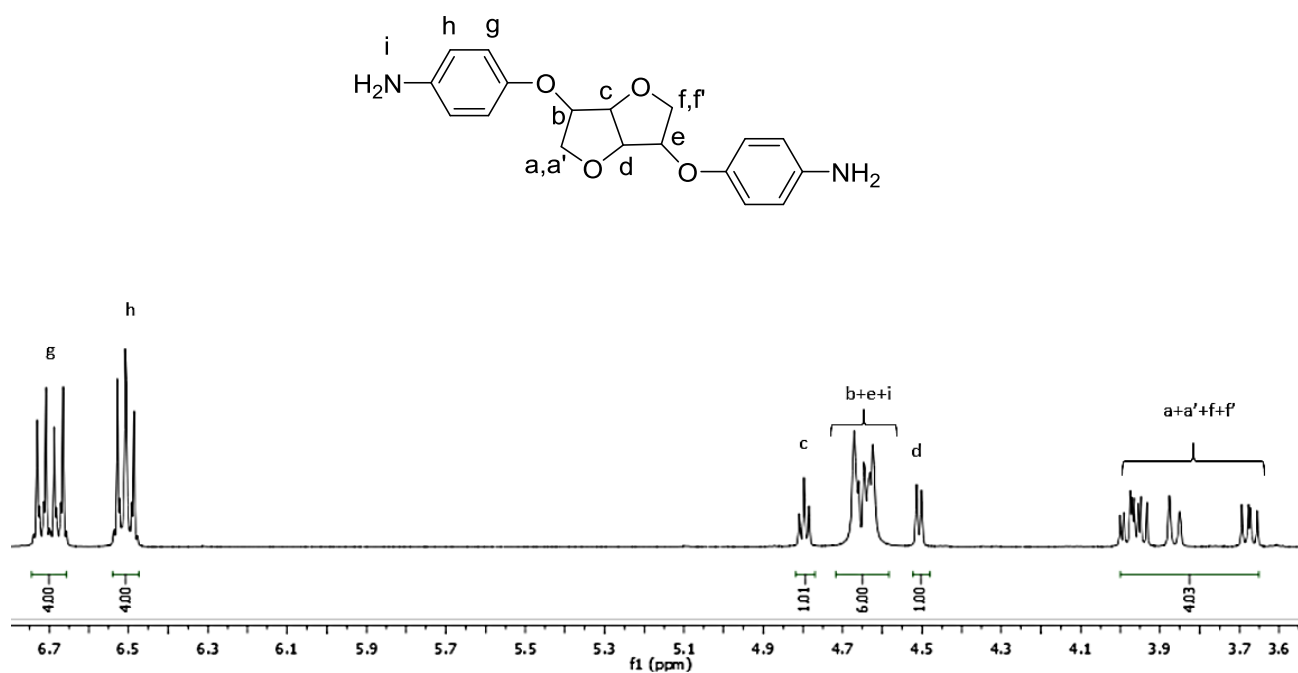


Figure S2. ^1H NMR spectrum of monomer 1b

^1H NMR (300 MHz, $\text{DMSO-}d_6$): δ (ppm): 4.1-3.65 (m, 4H); 4.50 (d, $J=3\text{Hz}$, 1H); 4.67-4.62 (m, 6H); 4.8 (t, $J=3\text{Hz}$, 1H); 6.54-6.48 (m, 4H) and 6.74-6.66 (m, 4H).

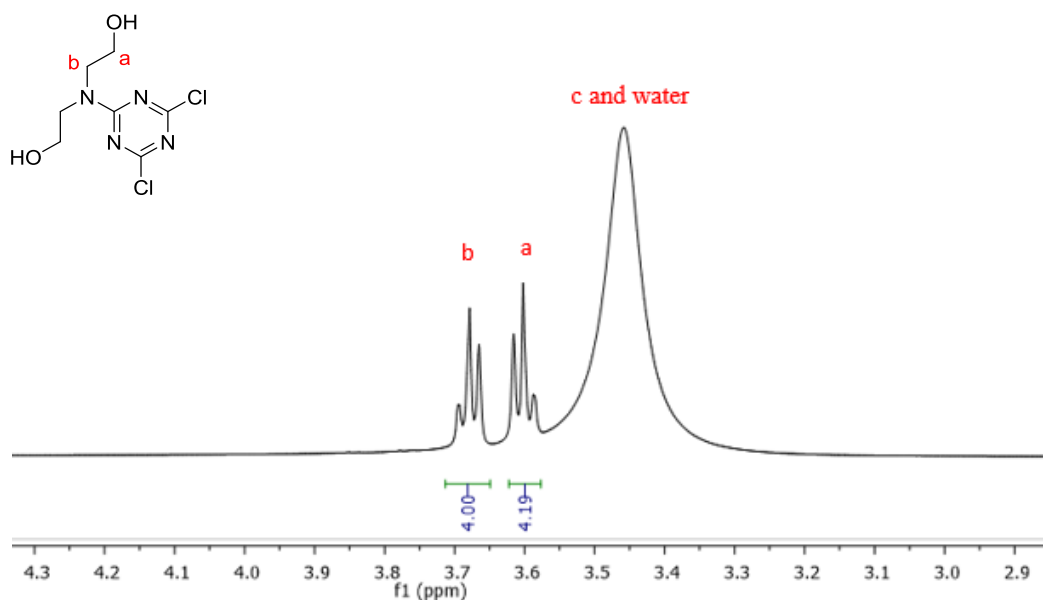


Figure S3. ^1H NMR spectrum of the monomer 2a

^1H NMR (300 MHz, $\text{DMSO-}d_6$): δ (ppm): 3.60 (t, $J=3\text{Hz}$, 4H) and 3.68 (t, $J=3\text{Hz}$, 4H).

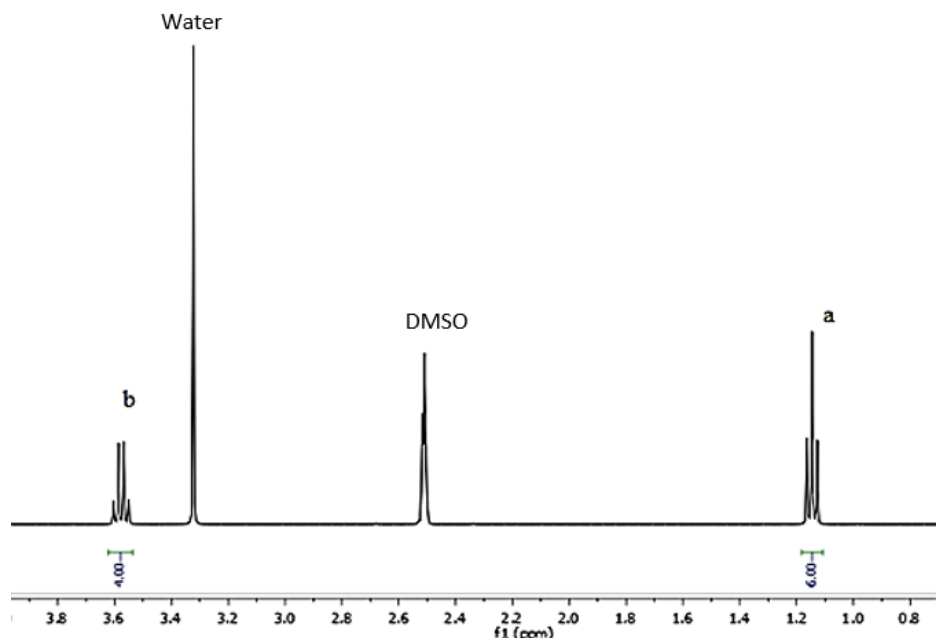
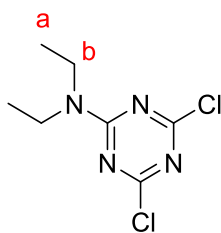


Figure S4. ^1H NMR spectrum of the monomer 2b

^1H NMR (300 MHz, $\text{DMSO-}d_6$): δ (ppm): 1.15 (t, $J=6\text{Hz}$, 6H) and 3.58 (q, $J=6\text{Hz}$, 4H)

NMR characterization of polymer P1-P5:

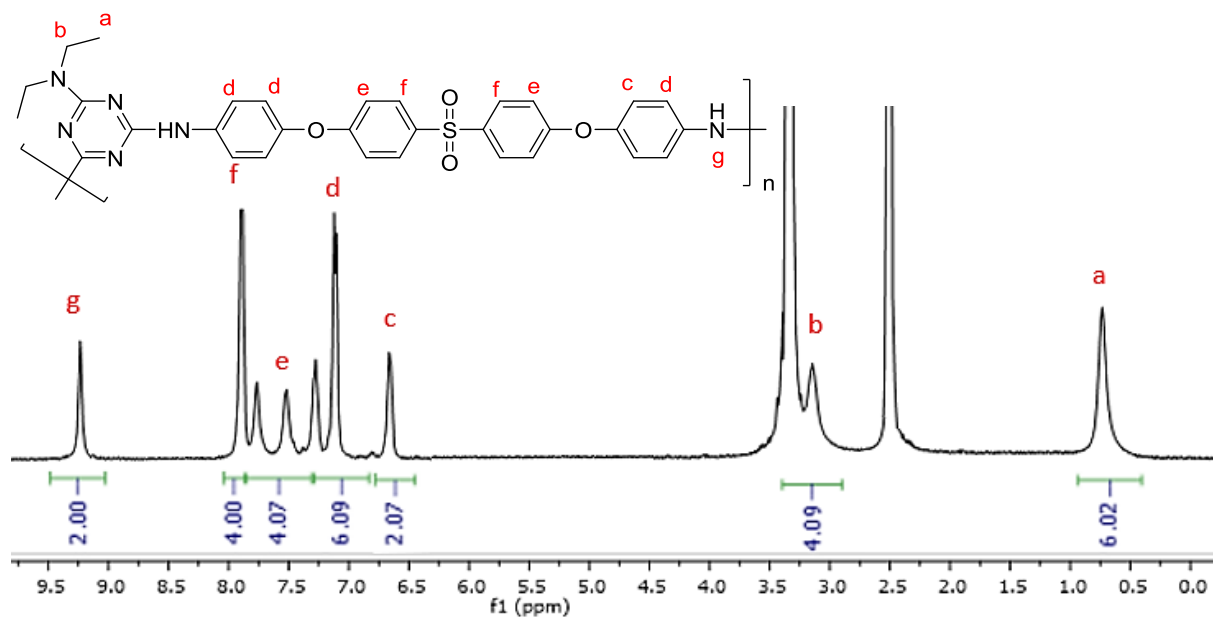


Figure S5. ¹H-NMR Spectrum of polymer P1

¹H NMR of polymer P1 (300 MHz, DMSO-*d*₆): δ (ppm): 0.86-0.66 (m, 6H); 3.23-3.02 (m, 4H); 6.67-6.65 (m, 2H); 7.28-7.10 (m, 6H); 7.77-7.52 (m, 4H); 7.90-7.88 (m, 4H) and 9.23 (s, 2H).

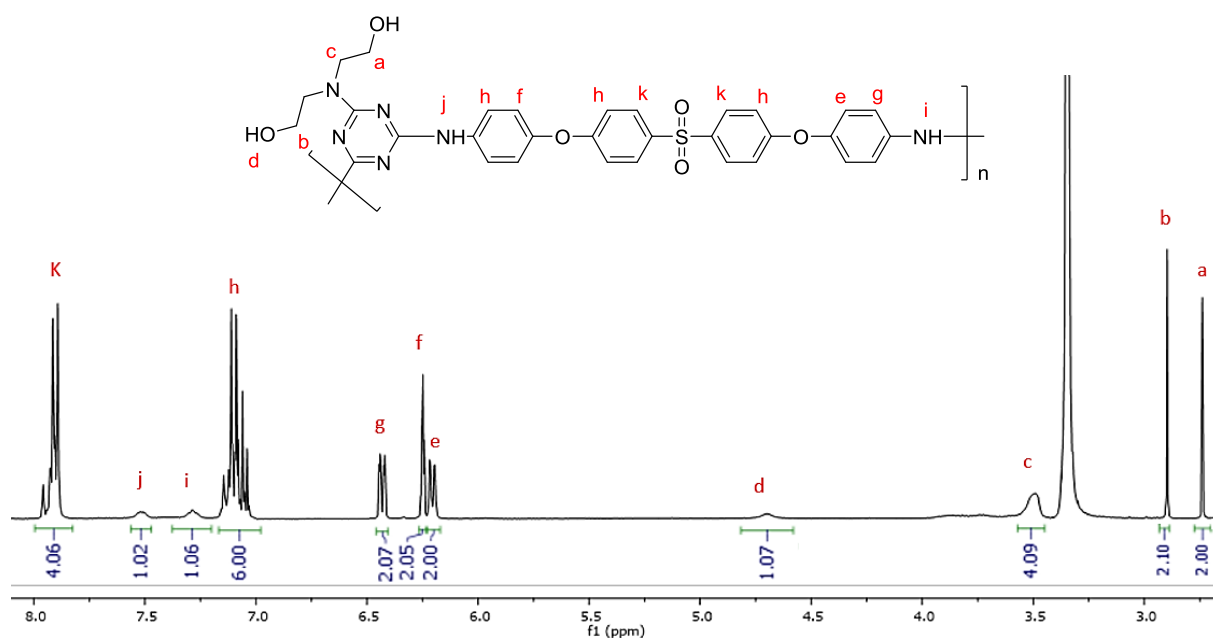


Figure S6. ¹H-NMR Spectrum of polymer P2

^1H NMR of polymer P2 (300 MHz, $\text{DMSO-}d_6$): δ (ppm): 2.73 (t, $J=3\text{Hz}$, 2H); 2.90 (t, $J=3\text{Hz}$, 2H); 3.53-3.41 (m, 4H); 4.70 (s, 1H); 6.22-6.19 (m, 2H); 6.26-6.24 (m, 2H); 6.45-6.40 (m, 2H); 7.12-7.09 (m, 6H); 7.54 (s, 1H); 7.29 (s, 1H) and 7.93-7.90 (m, 4H).

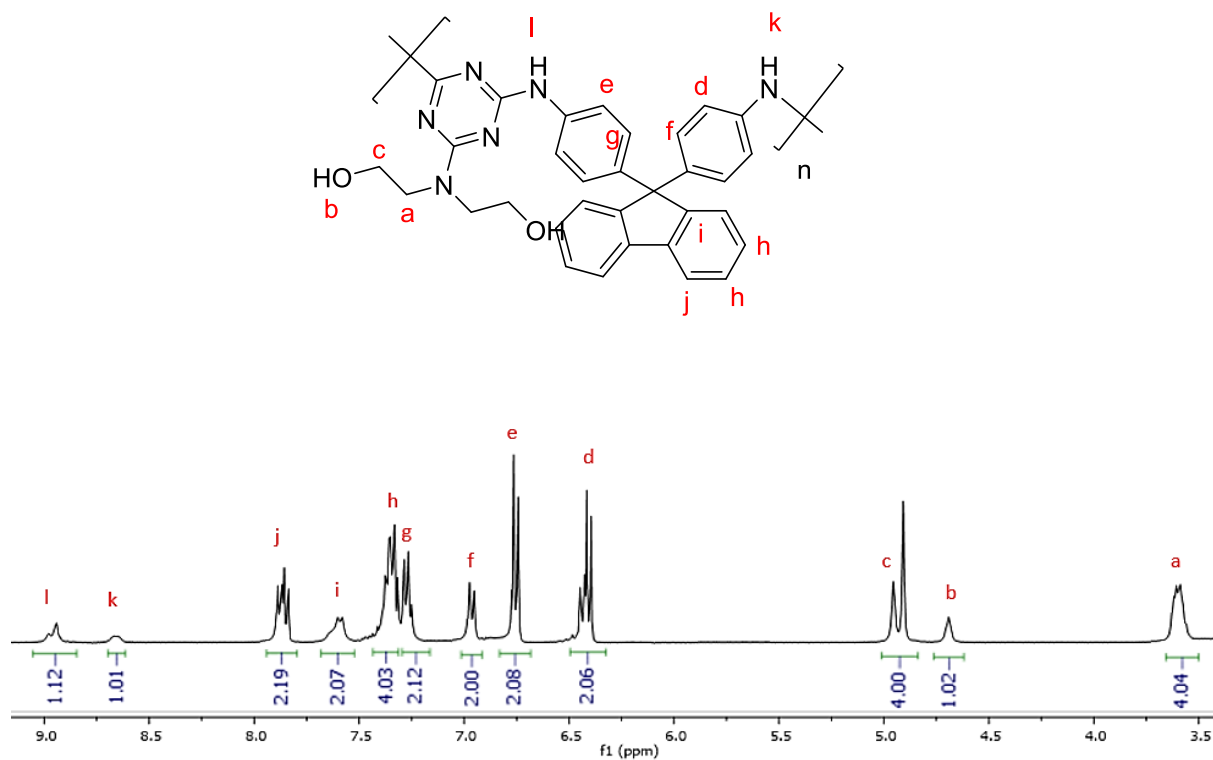


Figure S7. ^1H -NMR Spectrum of polymer P4

^1H NMR of polymer P4 (300 MHz, $\text{DMSO-}d_6$): δ (ppm): 3.67-3.59 (m, 4H); 4.69 (s, 1H); 4.96-4.91 (m, 4H); 6.46-6.39 (m, 2H); 6.77-6.75 (m, 2H); 6.97-6.95 (m, 2H); 7.29-7.25 (m, 2H); 7.38-7.33 (m, 4H); 7.60 (s, 2H); 7.89-7.84 (m, 2H); 8.72 (s, 1H) and 8.98 (s, 1H).

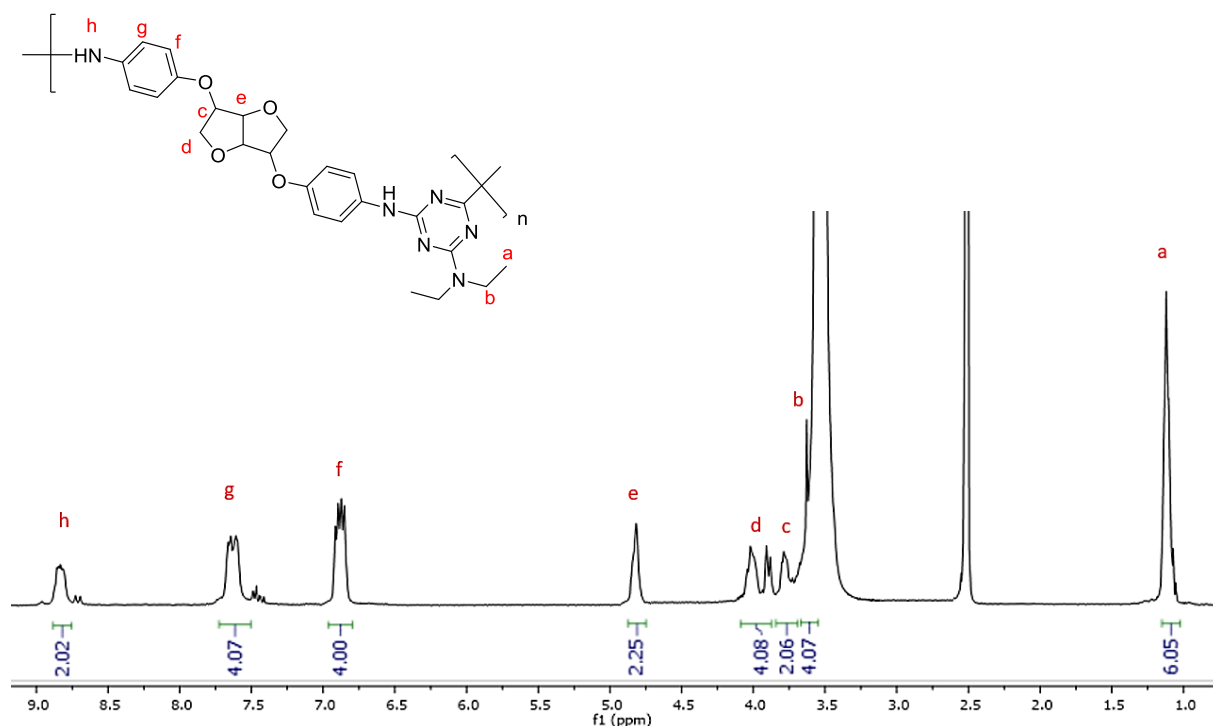


Figure S8. ^1H -NMR Spectrum of polymer P5

^1H NMR of polymer P5 (300 MHz, $\text{DMSO-}d_6$): δ (ppm): 1.13-1.07 (m, 6H); 3.68-3.60 (m, 4H); 3.82-3.72 (m, 2H); 4.04-3.87 (m, 4H); 4.83-4.79 (m, 2H); 6.91-6.84 (m, 4H); 7.66-7.61 (m, 4H) and 8.82 (s, 1H).

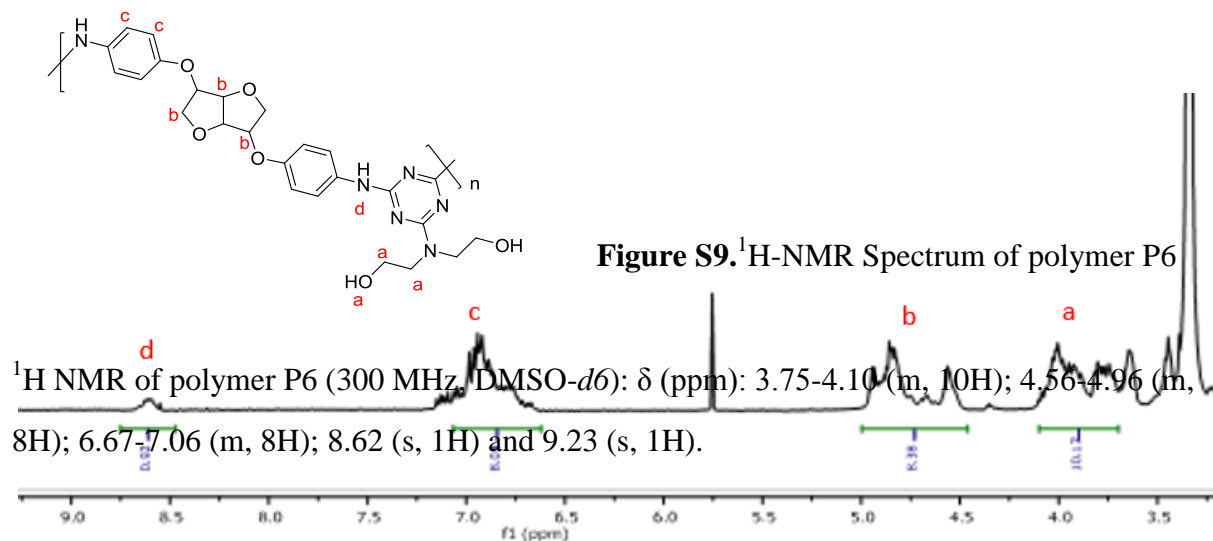


Figure S9. ^1H -NMR Spectrum of polymer P6

^1H NMR of polymer P6 (300 MHz, $\text{DMSO-}d_6$): δ (ppm): 3.75-4.10 (m, 10H); 4.56-4.96 (m, 8H); 6.67-7.06 (m, 8H); 8.62 (s, 1H) and 9.23 (s, 1H).